Sensing and Bio-Sensing Research 33 (2021) 100434

Contents lists available at ScienceDirect

Sensing and Bio-Sensing Research

journal homepage: www.elsevier.com/locate/sbsr

Flexible and wearable capacitive pressure sensor for blood pressure monitoring

Bijender [a,b], Ashok Kumar [a,b,*]

[a] CSIR-National Physical Laboratory, Dr. K. S. Krishnan Marg, Delhi 110012, India
[b] Academy of Scientific and Innovative Research (AcSIR), Ghaziabad 201002, India

ARTICLE INFO

Keywords:
Pressure sensor
PDMS
Blood pressure
Oscillometric waveform

ABSTRACT

A flexible pressure sensor based on a capacitive transduction mechanism having a polydimethylsiloxane (PDMS) layer incorporated between indium--tin-oxide (ITO) coated flexible polyethylene terephthalate (PET) electrodes has been developed. The sensor's key parameters have been improved by increasing the dielectric layer's porosity by introducing deionized water (DIW) into it. The sensing device with a porous dielectric layer (PDMS-DIW) exhibits a 0.07%–15% relative difference in capacitance for the applied pressure range from 1 Pa to 100 kPa. The device also demonstrates improved sensitivity compared to a PDMS layer (unstructured) throughout the complete external pressure range. The device with porous PDMS layer shows an extensive operating pressure range (1 Pa to 100 kPa), high working stability, quick response (≈110 ms) and ultra-low detection limit of pressure, i.e., 1 Pa. In addition, the blood pressure monitoring was also studied, and the devices gave a signature of the oscillometric waveform for different blood pressure (BP) values. The fabricated flexible pressure sensor can be used for wearable BP devices and biological applications due to its excellent functional properties.

1. Introduction

Due to high demands in electrical and electronic technologies for smart materials, artificial intelligence, industrial applications, robotic skin, and electronic skin[1–7], pressure sensors have been attracting significant attention among researchers working on various human physiological applications. In the last few years, several pressure sensors based on ceramic and polymer have been reported [8–11]; still, polymer-based flexible sensing devices have attracted main research focus because of their promising applications in human health-care monitoring devices [12–16], fingerprint sensors [17], energy harvesters [18–20], object detector [21], medical diagnostic tools [6,22] and so forth. Among various human health-care monitoring devices, blood pressure (BP) monitoring is the most common physiological parameter because blood pressure is a critical factor in identifying severe diseases related to the heart and kidney. High BP or hypertension is a vital sign for increasing the risk of stroke, heart failure, and kidney failure, and these diseases are the leading cause for increasing death in the world in the last few years [23,24]. Hence, blood pressure must be monitored regularly to identify early cardiovascular diseases, hypertension, heart rate, other vital human organ-related problems, etc.

The pressure sensors generate an electrical signal when external pressure is applied. The performance of any pressure sensor is evaluated by its key parameters like sensitivity, detection limit, operating pressure range, response time, and linearity. The pressure sensors operate in a signal transduction mechanism [25–27], and based on the transduction methods; sensors are usually categorized into three types, i.e., piezoresistive [28–33], piezocapacitive [13,34–37], and piezoelectric [38–45] pressure sensors. The piezoresistive pressure sensors transduced the change of resistance value into the output signal under the influence of external pressure [46], and piezoelectric pressure sensors work on the piezoelectric effect, which refers to the generation of electric charges when external pressure is applied. Out of these pressure sensors, the researchers commonly adopt capacitive-based sensing devices due to their several applications in wearable electronic devices, their outstanding performance, low-cost fabrication process, and simple structure. The sensors based on capacitive effect detected the change in capacitance value and transduced it into the output signal. The piezocapacitive pressure sensor works like a parallel-plate capacitor, and the capacitance of the capacitor is defined as

$$C = (\varepsilon \cdot A)/d$$

* Corresponding author at: CSIR-National Physical Laboratory, Dr. K. S. Krishnan Marg, Delhi 110012, India.
E-mail address: ashok553@nplindia.org (A. Kumar).

https://doi.org/10.1016/j.sbsr.2021.100434
Received 22 March 2021; Received in revised form 11 June 2021; Accepted 14 June 2021
Available online 17 June 2021

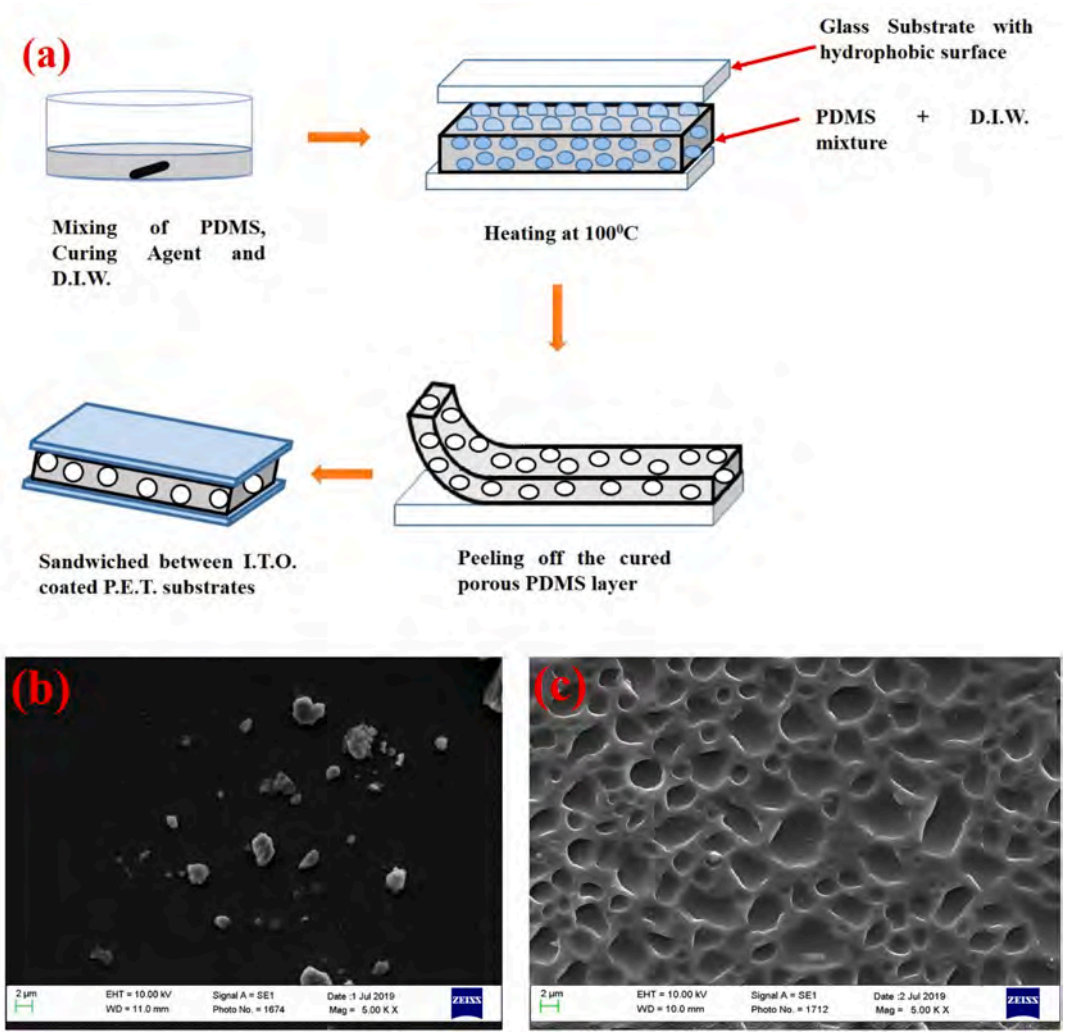

Fig. 1. Fabrication process and SEM characterization of PDMS and PDMS-DIW; (a) Overview of the process to fabricate the sensing device with a porous dielectric layer (PDMS-DIW). (b) Cross-sectional SEM image of the PDMS layer without DIW (c) Cross-sectional SEM image of the PDMS dielectric layer with DIW (Porous PDMS layer).

where ε is the absolute permittivity of the dielectric material, A and d represent the conducting plates' area and the distance between the parallel-plates. When external pressure is applied on capacitive pressure sensors, the thickness of the dielectric layer or the distance between the parallel conducting plates(d) changes, resulting in the change in the capacitance's value [47].

The functional materials play a vital role in developing sensing devices having high sensitivity and flexibility. The researchers used various functional materials to form the dielectric layer and flexible conducting electrodes to develop a capacitive-based pressure sensor. Among different functional materials, polydimethylsiloxane (PDMS) for dielectric layer and indium-tin-oxide (ITO) coated poly(ethylene terephthalate) (PET) substrates for flexible conducting electrodes are the best choice due to their high stability and flexibility. The PDMS structure can also be modified to enhance the pressure sensor's performance by improving their critical parameters like sensitivity, detection limit, response time, and so forth. We all need a pressure sensor with high sensitivity, and a large operating pressure range for the formation of wearable sensing devices. However, the researchers' big challenge is that some sensors exhibit high sensitivity but have a complicated fabrication process, low operating pressure range, and high energy consumption. However, many researchers developed flexible sensing devices with high sensitivity, quick response, and high working stability by altering the microstructure of the PDMS dielectric layer either by making the pores into it [13,48] or by incorporating scrubber into it [49] or by making it sponge [50] or by making micro-hyperboloids structure [51]. In this direction, we also improved the pressure sensor's key parameters by using deionized water (DIW) into the PDMS layer.

In today's life, blood pressure plays a crucial role in detecting cardiovascular diseases [52], which is the most common parameter for monitoring the human body's physiology. The oscillometric wave function required for clinical trials and development for the algorithm of automated non-invasive blood pressure monitoring devices required low-cost, highly sensitive pressure sensors [53]. Due to the requirement of highly sensitive flexible pressure sensor with a quick response in blood pressure monitoring devices, we have demonstrated a pressure sensing device based on a capacitive effect with a porous PDMS elastomer layer. The porous PDMS dielectric layer is developed by altering its structure by introducing DIW into it. The performance of the developed sensor under static and dynamic pressure has been investigated. Due to well-structured porosity, it shows improved vital parameters such as high sensitivity, low detection limit, quick response, and large operating pressure range. We have also explored the application of the developed sensor in blood pressure monitoring.

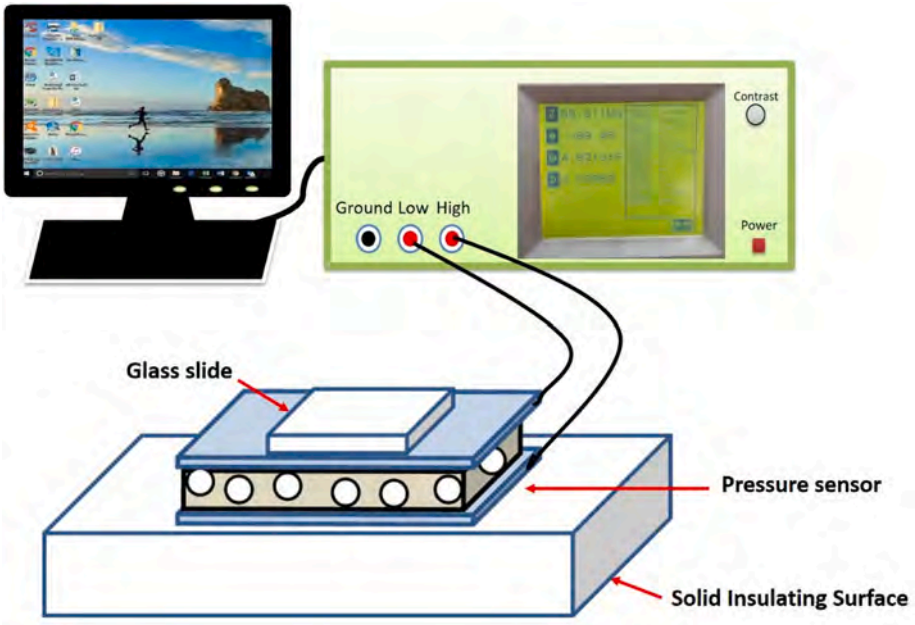

Fig. 2. Schematic illustration of the experimental arrangement for evaluating the difference in capacitance's values at various external pressure for the developed pressure sensor.

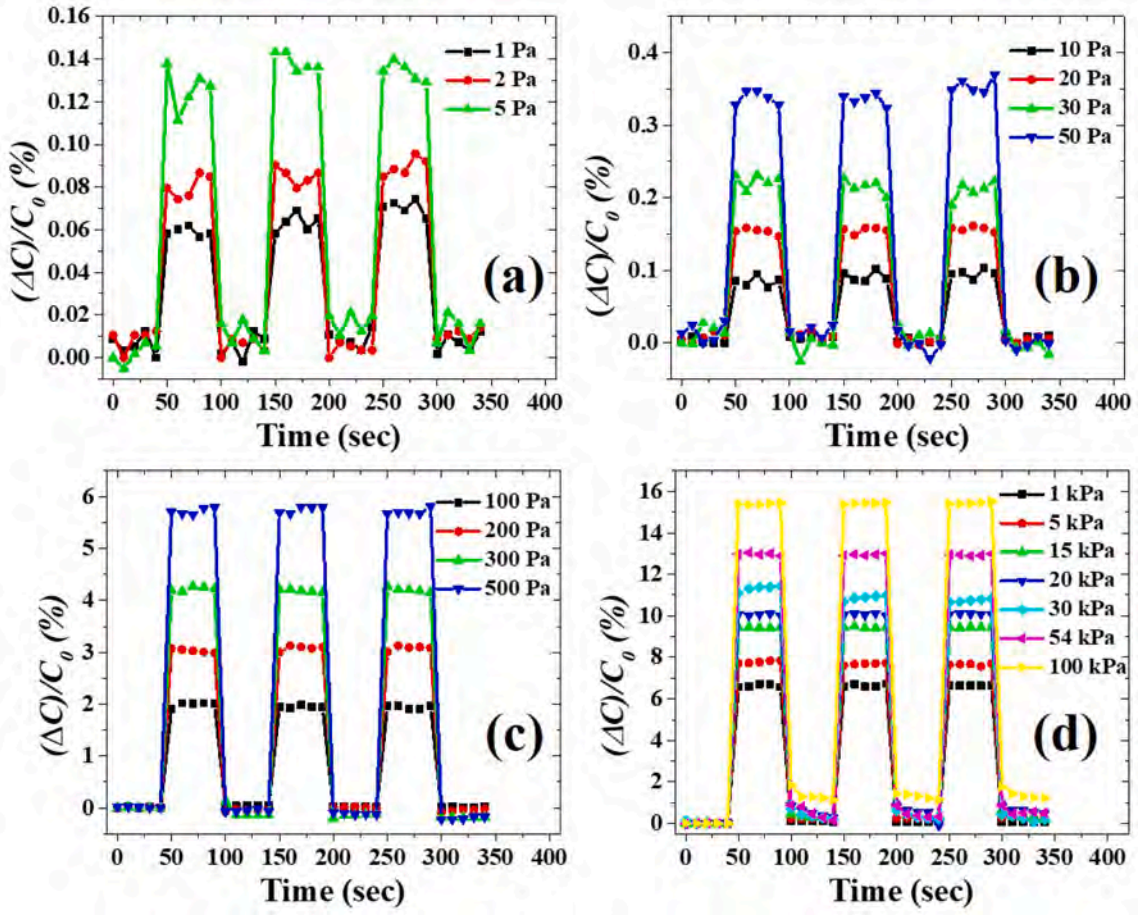

Fig. 3. The sensing performance of the developed sensor in terms of capacitance change at a different applied pressure range of (a) 1–5 Pa. (b) 10–50 Pa. (c) 100–500 Pa. (d) 1 kPa–100 kPa.

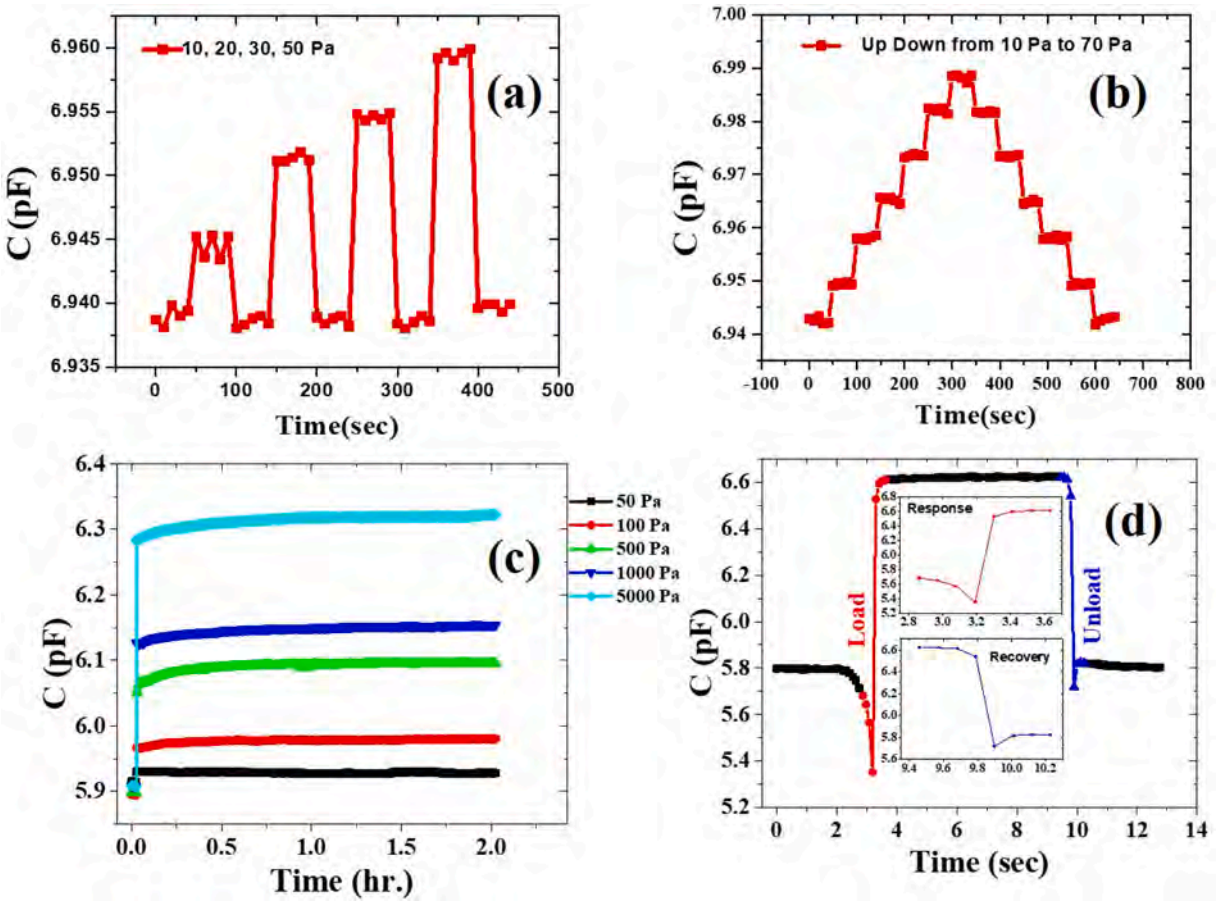

Fig. 4. Change in capacitance values versus time at step-wise change of external pressure (a) 10–50 Pa (b) Up Down from 10 Pa–70 Pa. (c) For a long time at 50 Pa, 100 Pa, 500 Pa, 1 kPa, and 5 kPa. (d) For calculating the response and recovery time of the fabricated sensor.

2. Experimental details

2.1. Fabrication of the porous dielectric layer and the pressure sensor

The fabrication process of a porous PDMS dielectric layer is illustrated in Fig. 1 (a). Polydimethylsiloxane (PDMS; Dow Corning Sylgard 184), a prepolymer, mixed with its curing agent in a weight ratio of 10:1. After mixing, deionized water (DIW) was added to the mixed solution in a weight ratio of 80:20 (PDMS: DIW). The solution of PDMS and DIW was mixed at 1000 rpm for 1 h by using a magnetic stirrer. For the fabrication of a dielectric layer of uniform thickness, the two glass slides were taken, and the glass slides were attached by using a spacer of the thickness of 1.2 mm. The mixed solution of PDMS and DIW was poured into the gap of 1.2 mm between the glass slides. For cross-linking between PDMS polymer, the assembled sample was annealed at 100 °C for 6 h, and during annealing, DIW present in the PDMS+DIW solution evaporates and leaves pores in the PDMS layer. The annealed porous PDMS layer was peeled off from the glass substrate and cut into a 20 mm × 20 mm piece from the cured sample for the characterization of electrical and sensing properties.

ITO coated PET substrates of 130 μm thickness were taken to sandwich the fabricated dielectric layer to form a flexible pressure sensor, and for the adhesion between substrates and the dielectric layer, a thin layer of PDMS solution was applied on the substrates. For the curing of PDMS adhesion layer, the whole sample was heated at 90 °C for 1 h, and the copper wires were attached to both sides of the conducting surface of the ITO coated flexible substrate for further measurements.

2.2. Characterization of porous PDMS layer and measurements

The presence of the porosity in the PDMS and porous PDMS (PDMS-DIW) dielectric layers was confirmed from the cross-sectional images using the scanning electron microscopy (SEM) technique as represented in Fig. 1 (c) & (d). A thin glass slide with a dimension of 12 mm × 12 mm of 555 mg weight was placed at the middle of the fabricated sensor having a 20 mm × 20 mm size to fix the effective area of the sample. The dead weights were used for applying static pressure on the glass slide, which is kept on the sample, as shown in Fig.3.

The variation of capacitance value at different applied pressure for the developed sensor was measured by the impedance analyzer (HIOKI 3532-50 LCR Hi-Tester) at 1 MHz frequency. The fabricated sensor was kept on the solid insulating surface to make a perfect difference in capacitance value. The static pressure was applied by loading and unloading dead weights at the middle of the developed sensing device to avoid disturbance during measurement. The well-defined blood pressure was generated on the pressure sensor sandwiched between the mandrel and the cuff using Fluke non-invasive blood pressure (NIBP) analyzer.

3. Results and discussion

The porous PDMS dielectric layer was formed by mixing DIW in the PDMS layer, and the developed porous PDMS layer was sandwiched between the flexible electrodes, as shown in Fig. 1 (a). The detailed fabrication process of the designed device is given in the experimental section. The porosity in the PDMS and PDMS –DIW (porous PDMS) layer was identified by cross-sectional SEM images, as illustrated in Fig. 1 (b & c). Fig. 1(b) represents the cross-sectional SEM image of the pure PDMS

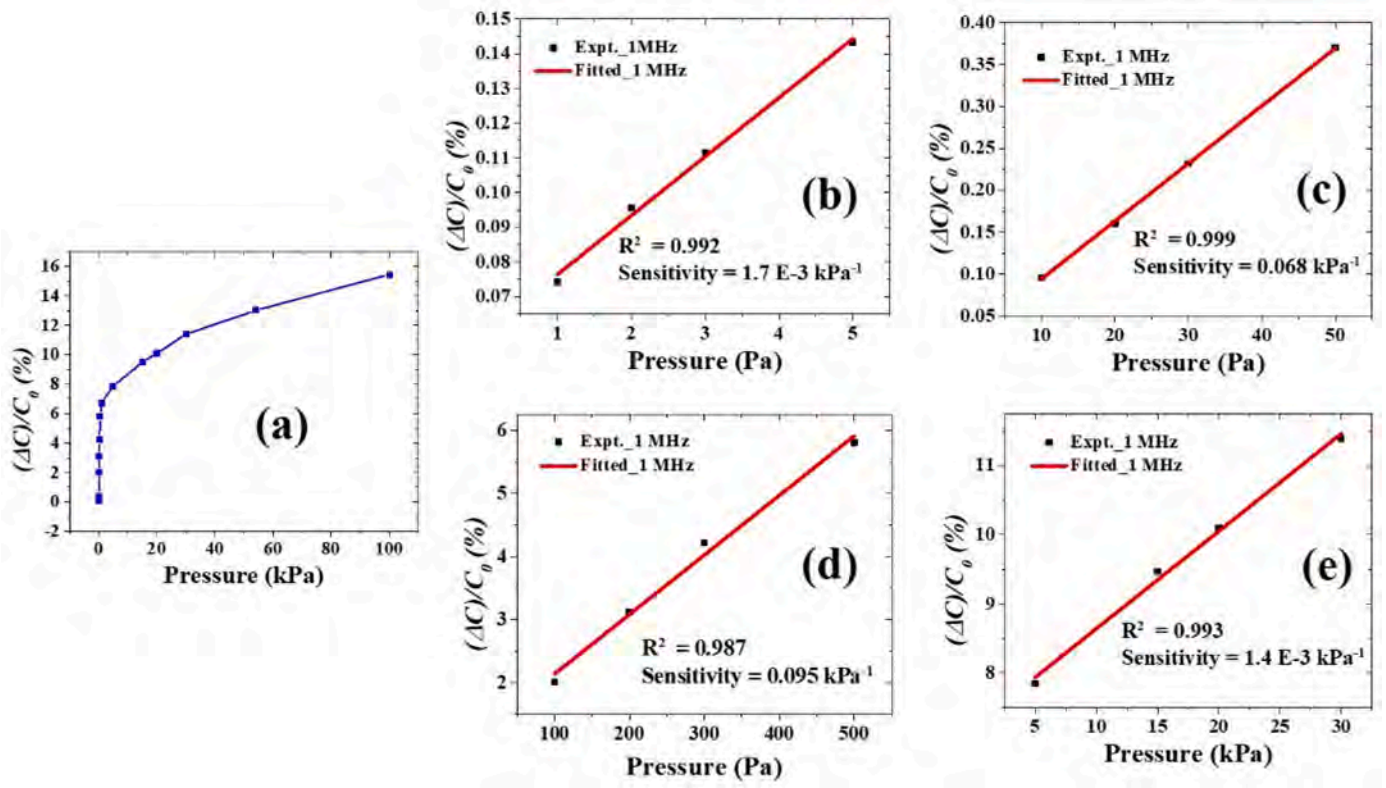

Fig. 5. The relative difference in capacitance versus the external pressure at different regions of (a) 10 Pa–100 kPa (b) 1–5 Pa. (c) 10–50 Pa. (d) 100–500 Pa. (e) 5 kPa–30 kPa.

layer, which shows no porosity present in the layer. Similarly, Fig. 1(c) illustrates the cross-sectional SEM image of the cured-porous PDMS layer, which shows a well-defined cross-net structure representing the well-defined network of void in the bulk PDMS structure. The developed voids/porosities create significant changes in the pressure sensor's capacitance in dynamic or static pressure conditions.

The capacitance response for the developed sensor with PDMS and porous PDMS layer was measured by applying the external pressure using dead weights, as described in Section 2.2. The applied pressure value depends on the value of force and the area of the sensor. Here, the sensing device's effective area was fixed by putting a thin glass slide of dimension 12 mm × 12 mm on it. After fixing the device area, the external pressure depends only on the force applied by the dead weights, which were made according to the glass slide's dimensions. The relative difference in capacitance ($\Delta C/C_0$, where $\Delta C = C - C_0$; C_0 is the capacitance's value of the sensor without any external pressure) versus time was measured by varying external pressure ranging from 1 Pa to 100 kPa. The experimental arrangement for evaluating the change in capacitance's value is illustrated in Fig. 2. The pressure sensor electrodes are attached to the LCR meter to obtain the capacitance, reactance, and other vital electrical parameters for a possible electronic digital display unit.

The sensing device having a porous PDMS dielectric layer detects ultra-low pressure of 1 Pa and gives approx. 0.07% relative change in capacitance as illustrated in Fig. 3 (a). Similarly, the relative change in capacitance increased with increasing the applied pressure from 1 Pa to 100 kPa, as shown in Fig. 3. The sensor gives a maximum of 15% relative difference in capacitance for a pressure of 100 kPa. The sensing device having a PDMS layer (PDMS without DIW) detects the lowest pressure of 10 Pa and gives approx. 0.03% & only 3.01% relative difference in capacitance for external pressure of 10 Pa and 100 kPa, respectively.

The change in capacitance versus time at step-wise change of external pressure was also measured for the sensor having a porous PDMS layer to confirm the device's repeatability, as shown in Fig. 4 (a & b). In Fig. 4 (a), the change in capacitance values was measured by putting different dead-weights for applying the pressure of 10 Pa, 20 Pa, 30 Pa, and 50 Pa, whereas in Fig. 4(b), the capacitance values were measured at different external pressure, which was applied by putting weights on one another from 10 Pa to 70 Pa and in reverse from 70 Pa to 10 Pa by lifting the weights one by one. The fabricated sensor also shows a linear response for step-wise external pressure change, as illustrated in Fig. 4 (a & b).

The developed sensor's operational stability was also checked by applying different pressure for a long time (for 2 h), as shown in Fig. 4 (c). The change in the capacitance value remained constant for 2 h at each applied pressure, i.e. 50 Pa, 100 Pa, 500 Pa, 1 kPa, and 5 kPa. The response time during loading and recovery time during unloading is shown in Fig. 4 (d). The device's capacitance was immediately changed from 5.8 pF to 6.6 pF within 110 ms under the application of an external pressure of 500 Pa. When the pressure was removed, the sensor gains its initial capacitance value in the same time interval (inset of Fig. 4 (d), the sensor shows the response and recovery time of 110 ms).

The sensitivity (S) of the fabricated sensing devices was calculated by the slope of the relative change in capacitance versus the applied external pressure. The sensitivity of the pressure sensor (S) is defined as the ratio of variation in the relative change in capacitance and the applied external pressure [13], i.e. $S = \delta(\Delta C/C_0)/\delta P$.

The graph between relative change in capacitance and the applied pressure (ranging from 1 Pa–100 kPa) is shown in Fig. 5 (a). The pressure points/range was selected for various regions depending on the requirement of measuring pressure, i.e. first pressure region (1–5 Pa), second pressure region (10 Pa – 50 Pa), third pressure region (100 Pa–500 Pa), and fourth pressure region (5 kPa–30 kPa). The fabricated device with the PDMS-DIW layer has a linear response in all pressure regions. The sensitivity of the developed sensor was found 1.7 E−3 kPa^{-1} (Fig. 5 (b)), 0.068 kPa^{-1} (Fig. 5 (c)), 0.095 kPa^{-1} (Fig. 5 (d)), and

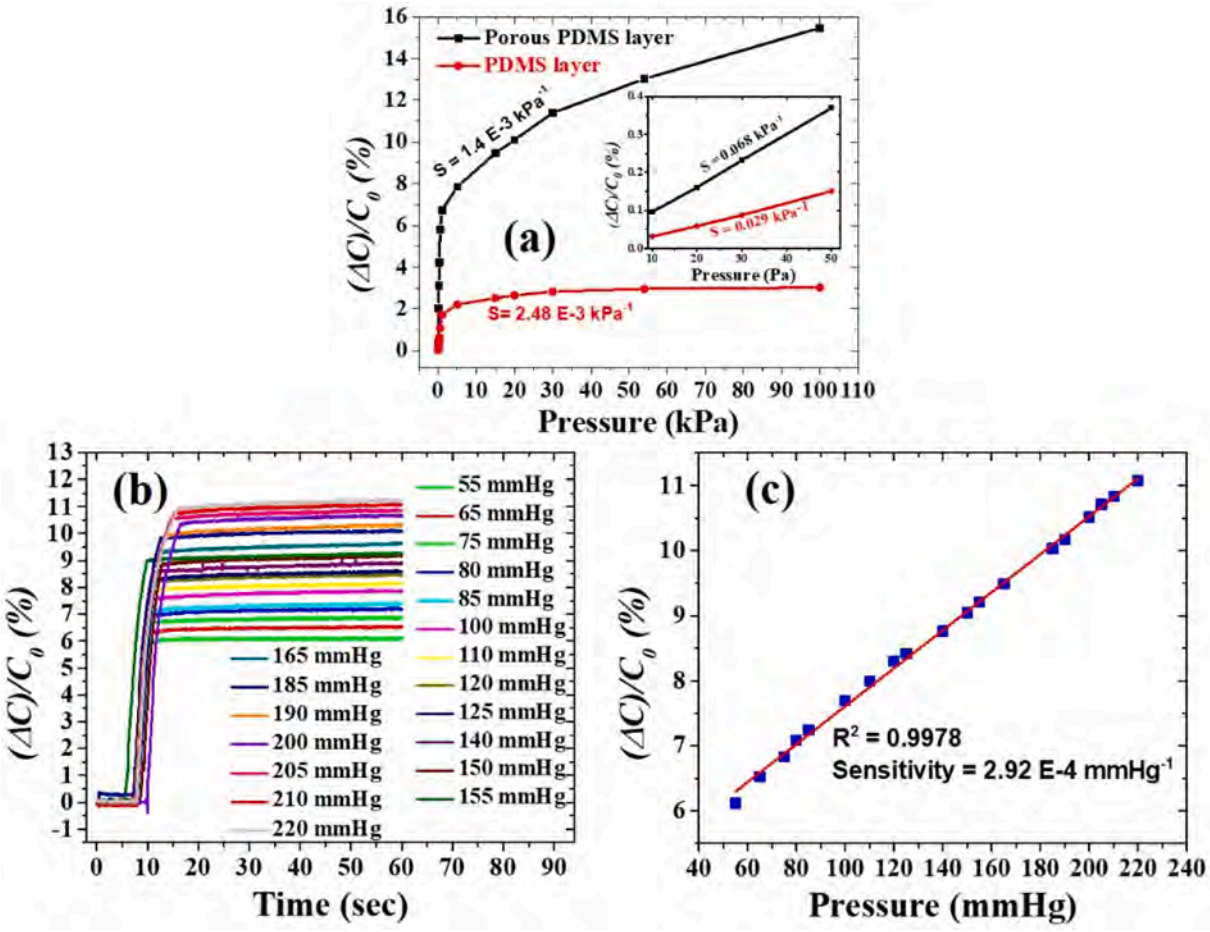

Fig. 6. (a) Comparison between the pressure sensors' sensing performance having PDMS-DIW (Porous PDMS) and PDMS dielectric layer. (b) The relative difference in capacitance versus time at various static pressure ranges from 55 mmHg to 220 mmHg using the NIBP analyzer. (c) Variation of the relative difference in capacitance with applied pressure ranges from 55 mmHg to 220 mmHg.

Table 1
Comparison between the capacitive pressure sensors based on PDMS microstructure.

Transduction mechanism	Material/structure	Sensitivity (Pressure range)	Response/ Recover time	Minimum detection	References
Capacitive	PDMS/Wrinkled microstructure	0.0012 kPa^{-1} (<1 kPa) 4.2 E−6 kPa^{-1} (>8 kPa)	578/782 ms	NA	[36]
Capacitive	Porous PDMS	0.26 kPa^{-1} (0–0.33 kPa) 0.01 kPa^{-1} (0.33–250 kPa)	15/−ms	1 Pa	[13]
Capacitive	Porous PDMS	0.046 kPa^{-1} (0.01–0.05 kPa) 0.051 kPa^{-1} (0.1–0.5 kPa)	NA	5 Pa	[49]
Capacitive	Bubble trapped PDMS	5.5 E−3 kPa^{-1} (0–10.20 kPa)	~351/386 ms	NA	[54]
Capacitive	**PDMS/DIW**	**0.068 kPa^{-1}(0.01–0.05 kPa)** **0.095 kPa^{-1}(0.1–0.5 kPa)**	**~110/110 ms**	**1 Pa**	**This Work**

1.4 E−3 kPa^{-1} (Fig. 5 (e)) in 1st, 2nd, 3rd and 4th pressure regions, respectively. One can construct a new pressure range and calculate its sensitivity depending on the measurement pressure.

A comparison between the sensitivities of the devices having PDMS layer (PDMS without DIW) and porous PDMS (PDMS with DIW) layer was studied, and it was found that the sensitivity of the device with PDMS-DIW layer was significantly improved compared to the device having PDMS layer in 2nd (inset of Fig. 6 (a)) and 4th pressure regions as shown in Fig. 6 (a).

Due to the improved sensitivity of the developed device with porous PDMS layer in the 4th pressure region, the device was tested by applying static pressure in the pressure range of 55 mmHg to 220 mmHg to explore its suitability for monitoring human blood pressure. The developed device was attached to the mandrel, and a cuff was wrapped over it, which is connected with Fluke NIBP analyzer by which the static pressure was applied. The change in capacitance values was different for every static pressure value, as shown in Fig. 6(b) and the sensor has a linear response with a sensitivity of 2.92 E−4 $mmHg^{-1}$ in the applied static pressure range of 55 mmHg to 220 mmHg, as shown in Fig. 6(c). A comparison chart of various capacitive pressure sensors based on PDMS microstructure pattern is given in Table 1, which shows that the sensor reported in this article showed high sensitivity and ultra-low detection limit.

Blood pressure (BP) monitoring for different BP ranges was performed after getting the good sensitivity under static pressure in the blood pressure range (from 55 mmHg to 220 mmHg). The flexible pressure sensor was sandwiched between the mandrel (act as an artificial human hand) and cuff; the cuff was connected with the OMRON BP

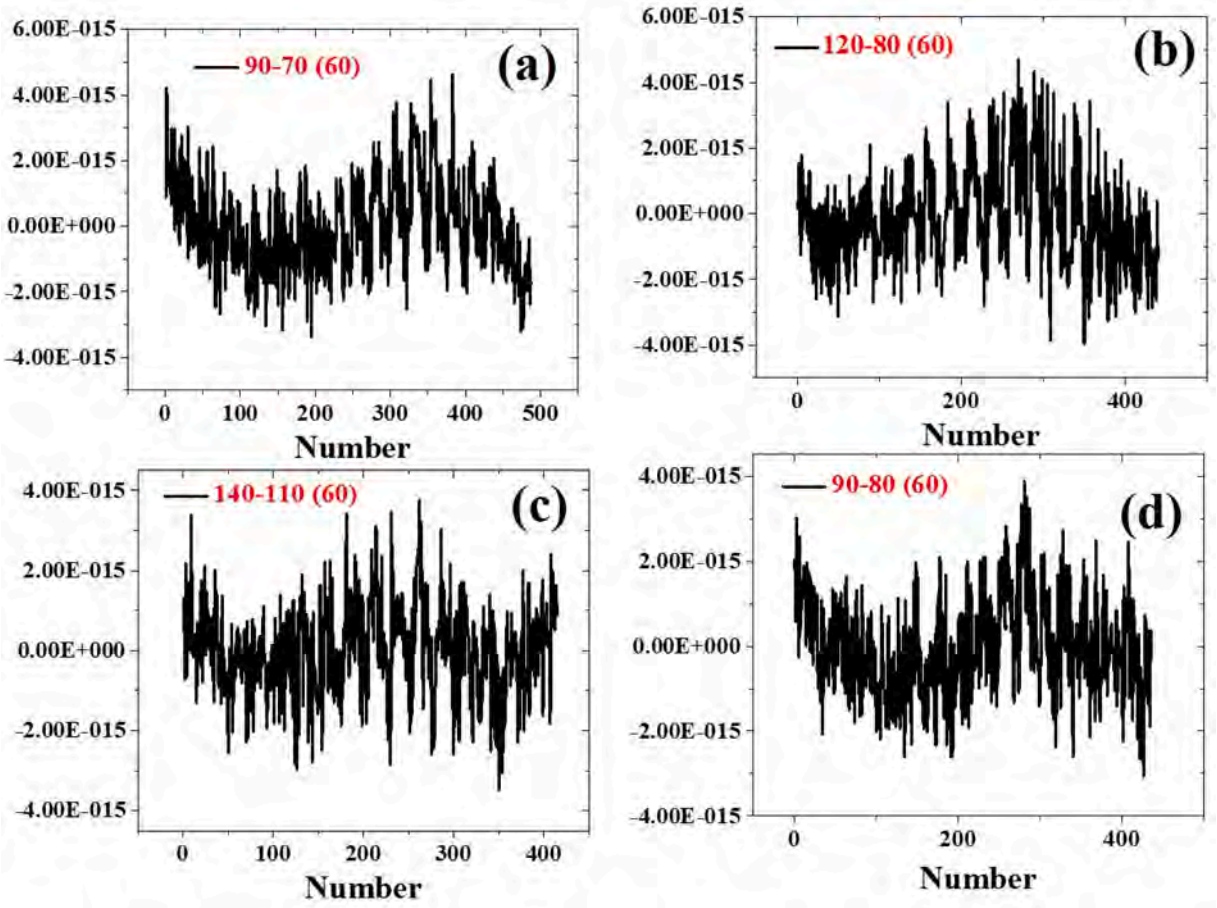

Fig. 7. Human blood pressure (BP) monitoring of the fabricated sensor at different BP values with the heartbeat of 60 BPM. (a) For low BP value. (b) For Normal BP value. (c) For high BP value. (d) For BP value of 90–80.

machine and also combined with the Fluke NIBP analyzer, and the output was taken in terms of capacitance value by using LCR meter.

The pressure was applied to the cuff wrapped on the mandrel by the OMRON BP machine. The BP machine started applying pressure in the cuff; simultaneously, the pulse having systolic- diastolic value with 60 beats per minute (BPM) was given by the Fluke NIBP analyzer on the mandrel. The pressure sensing device shows an entire curve in terms of capacitance values starting from applying the pressure, deflation curve, and releasing pressure from the cuff. The deflation pressure curve was extracted from the pressure generated by the BP machine and the oscillometric waveform produced by the NIBP analyzer. The variation of capacitance was the overlapping of two curves; the first curve was due to the pressure of the cuff, and the second curve was due to the human pulse given by the NIBP analyzer. The human pulse waveform was extracted from the deflation curve, also known as an oscillometric waveform, as shown in Fig. 7 (a–d). Our low-cost pressure sensor gives a well defined signature of the oscillometric waveform for different BP ranges (i.e. normal, low and high) and shows their potential for other biological applications. However, we have to improve further the developed sensor's sensitivity for getting well resolved oscillometric waveform. In the future, we will improve its sensitivity by further altering the structure of the PDMS layer and explore their applications in wearable electronic devices.

4. Conclusion

We have fabricated capacitive flexible pressure sensors with a porous (PDMS-DIW) dielectric layer over a large operating pressure range (from 1 Pa to 100 kPa). The PDMS-DIW layer device's pressure sensitivity was remarkably improved compared to the device with only the PDMS layer. The device shows the sensitivity of 1.7 E−3 kPa^{-1} in the pressure range of 1–5 Pa, 0.068 kPa^{-1} in the pressure range of 10–50 Pa, 0.095 kPa^{-1} in the pressure range of 100–500 Pa, and 1.4 E−3 kPa^{-1} in the pressure range of 5–30 kPa, respectively. The pressure sensor maintains its stability for a long time measurement at different applied pressure and responds quickly during loading/unloading of dead weights with a response and recovery time of nearly 110 ms. Due to its improved sensitivity and quick response, the NIBP analyzer was used to detect the oscillometric wave form of known systolic and diastolic pressure. The developed sensor showed their potential to use as human health-care devices and wearable electronic devices.

Declaration of Competing Interest

The authors declare that they have no known competing financial interests or personal relationships that could have appeared to influence the work reported in this paper.

Acknowledgments

The authors would like to thank the Director, CSIR-NPL, Head, Physico-Mechanical Metrology division, CSIR-NPL, for their support and constant encouragement. Mr. Bijender thanks AcSIR for pursuing a Ph.D. program and also wants to thank Mr. Shubham Kumar for his constant help and support.

References

[1] N. Lu, D.-H. Kim, Flexible and stretchable electronics paving the way for soft robotics, Soft Robot. 1 (2014) 53–62, https://doi.org/10.1089/soro.2013.0005.

[2] C. Majidi, Soft robotics: a perspective—current trends and prospects for the future, Soft Robot. 1 (2014) 5–11, https://doi.org/10.1089/soro.2013.0001.

[3] W.-Y. Chang, C.-C. Chen, C.-C. Chang, C.-L. Yang, An enhanced sensing application based on a flexible projected capacitive-sensing mattress, Sensors. 14 (2014) 6922–6937, https://doi.org/10.3390/s140406922.

[4] W.-Y. Chang, T.-H. Fang, S.-H. Yeh, Y.-C. Lin, Flexible electronics sensors for tactile multi-touching, Sensors. 9 (2009) 1188–1203, https://doi.org/10.3390/s9021188.

[5] A. Kang, J. Lin, X. Ji, W. Wang, H. Li, C. Zhang, T. Han, A high-sensitivity pressure sensor based on surface transverse wave, Sensors Actuators A Phys. 187 (2012) 141–146, https://doi.org/10.1016/j.sna.2012.08.017.

[6] G. Schwartz, B.C.K. Tee, J. Mei, A.L. Appleton, D.H. Kim, H. Wang, Z. Bao, Flexible polymer transistors with high pressure sensitivity for application in electronic skin and health monitoring, Nat. Commun. 4 (2013) 1859, https://doi.org/10.1038/ncomms2832.

[7] X. Wang, Y. Gu, Z. Xiong, Z. Cui, T. Zhang, Silk-molded flexible, ultrasensitive, and highly stable electronic skin for monitoring human physiological signals, Adv. Mater. 26 (2014) 1336–1342, https://doi.org/10.1002/adma.201304248.

[8] V.N. Thakur, A. Zafer, S. Yadav, A. Kumar, Ferroelectric-dielectric composite pressure sensor, Sensors Actuators A Phys. 297 (2019) 111536, https://doi.org/10.1016/j.sna.2019.111536.

[9] V.N. Thakur, B.P. Singh, S. Yadav, A. Kumar, Giant pressure sensitivity in piezo/ferro-electric ceramics, RSC Adv. 10 (2020) 9140–9145, https://doi.org/10.1039/D0RA00484G.

[10] V.N. Thakur, S. Yadav, A. Kumar, Effect of bismuth substitution on piezoelectric coefficients and temperature and pressure-dependent dielectric and impedance properties of lead zirconate titanate ceramics, Mater. Today Commun. 101846 (2020), https://doi.org/10.1016/j.mtcomm.2020.101846.

[11] C. Singh, V.N. Thakur, A. Kumar, Investigation on barometric and hydrostatic pressure sensing properties of Pb[(Mg1/3Nb2/3)0.7Ti0.3]O3 electro-ceramics, Ceram. Int. 47 (2021) 6982–6987, https://doi.org/10.1016/j.ceramint.2020.11.047.

[12] F. Xu, X. Li, Y. Shi, L. Li, W. Wang, L. He, R. Liu, Recent developments for flexible pressure sensors: a review, Micromachines. 9 (2018) 580, https://doi.org/10.3390/mi9110580.

[13] S. Chen, B. Zhuo, X. Guo, Large area one-step facile processing of microstructured elastomeric dielectric film for high sensitivity and durable sensing over wide pressure range, ACS Appl. Mater. Interfaces 8 (2016) 20364–20370, https://doi.org/10.1021/acsami.6b05177.

[14] Y. Khan, A.E. Ostfeld, C.M. Lochner, A. Pierre, A.C. Arias, Monitoring of vital signs with flexible and wearable medical devices, Adv. Mater. 28 (2016) 4373–4395, https://doi.org/10.1002/adma.201504366.

[15] D. Kwon, T.-I. Lee, J. Shim, S. Ryu, M.S. Kim, S. Kim, T.-S. Kim, I. Park, Highly sensitive, flexible, and wearable pressure sensor based on a giant piezocapacitive effect of three-dimensional microporous elastomeric dielectric layer, ACS Appl. Mater. Interfaces 8 (2016) 16922–16931, https://doi.org/10.1021/acsami.6b04225.

[16] B. Nie, R. Li, J. Cao, J.D. Brandt, T. Pan, Flexible transparent iontronic film for interfacial capacitive pressure sensing, Adv. Mater. 27 (2015) 6055–6062, https://doi.org/10.1002/adma.201502556.

[17] N. Sato, S. Shigematsu, H. Morimura, M. Yano, K. Kudou, T. Kamei, K. Machida, Novel surface structure and its fabrication process for MEMS fingerprint sensor, IEEE Trans. Electron Devices. 52 (2005) 1026–1032, https://doi.org/10.1109/TED.2005.846342.

[18] Y. Yang, H. Zhang, Z.-H. Lin, Y.S. Zhou, Q. Jing, Y. Su, J. Yang, J. Chen, C. Hu, Z. L. Wang, Human skin based triboelectric nanogenerators for harvesting biomechanical energy and as self-powered active tactile sensor system, ACS Nano 7 (2013) 9213–9222, https://doi.org/10.1021/nn403838y.

[19] G. Zhu, W.Q. Yang, T. Zhang, Q. Jing, J. Chen, Y.S. Zhou, P. Bai, Z.L. Wang, Self-powered, ultrasensitive, flexible tactile sensors based on contact electrification, Nano Lett. 14 (2014) 3208–3213, https://doi.org/10.1021/nl5005652.

[20] S. Wang, L. Lin, Z.L. Wang, Triboelectric nanogenerators as self-powered active sensors, Nano Energy 11 (2015) 436–462, https://doi.org/10.1016/j.nanoen.2014.10.034.

[21] C. Metzger, E. Fleisch, J. Meyer, M. Dansachmüller, I. Graz, M. Kaltenbrunner, C. Keplinger, R. Schwödiauer, S. Bauer, Flexible-foam-based capacitive sensor arrays for object detection at low cost, Appl. Phys. Lett. 92 (2008), 013506, https://doi.org/10.1063/1.2830815.

[22] Y. Zang, F. Zhang, C. Di, D. Zhu, Advances of flexible pressure sensors toward artificial intelligence and health care applications, Mater. Horizons. 2 (2015) 140–156, https://doi.org/10.1039/C4MH00147H.

[23] S.S. Lim, T. Vos, A.D. Flaxman, G. Danaei, K. Shibuya, H. Adair-Rohani, M. Amann, H.R. Anderson, K.G. Andrews, M. Aryee, C. Atkinson, L.J. Bacchus, A.N. Bahalim, K. Balakrishnan, J. Balmes, S. Barker-Collo, A. Baxter, M.L. Bell, J.D. Blore, F. Blyth, C. Bonner, G. Borges, R. Bourne, M. Boussinesq, M. Brauer, P. Brooks, N. G. Bruce, B. Brunekreef, C. Bryan-Hancock, C. Bucello, R. Buchbinder, F. Bull, R. T. Burnett, T.E. Byers, B. Calabria, J. Carapetis, E. Carnahan, Z. Chafe, F. Charlson, H. Chen, J.S. Chen, A.T.A. Cheng, J.C. Child, A. Cohen, K.E. Colson, B.C. Cowie, S. Darby, S. Darling, A. Davis, L. Degenhardt, F. Dentener, D.C. Des Jarlais, K. Devries, M. Dherani, E.L. Ding, E.R. Dorsey, T. Driscoll, K. Edmond, S.E. Ali, R. E. Engell, P.J. Erwin, S. Fahimi, G. Falder, F. Farzadfar, A. Ferrari, M.M. Finucane, S. Flaxman, F.G.R. Fowkes, G. Freedman, M.K. Freeman, E. Gakidou, S. Ghosh, E. Giovannucci, G. Gmel, K. Graham, R. Grainger, B. Grant, D. Gunnell, H. R. Gutierrez, W. Hall, H.W. Hoek, A. Hogan, H.D. Hosgood, D. Hoy, H. Hu, B. J. Hubbell, S.J. Hutchings, S.E. Ibeanusi, G.L. Jacklyn, R. Jasrasaria, J.B. Jonas, H. Kan, J.A. Kanis, N. Kassebaum, N. Kawakami, Y.H. Khang, S. Khatibzadeh, J. P. Khoo, C. Kok, F. Laden, R. Lalloo, Q. Lan, T. Lathlean, J.L. Leasher, J. Leigh, Y. Li, J.K. Lin, S.E. Lipshultz, S. London, R. Lozano, Y. Lu, J. Mak, R. Malekzadeh, L. Mallinger, W. Marcenes, L. March, R. Marks, R. Martin, P. McGale, J. McGrath, S. Mehta, G.A. Mensah, T.R. Merriman, R. Micha, C. Michaud, V. Mishra, K. M. Hanafiah, A.A. Mokdad, L. Morawska, D. Mozaffarian, T. Murphy, M. Naghavi, B. Neal, P.K. Nelson, J.M. Nolla, R. Norman, C. Olives, S.B. Omer, J. Orchard, R. Osborne, B. Ostro, A. Page, K.D. Pandey, C.D.H. Parry, E. Passmore, J. Patra, N. Pearce, P.M. Pelizzari, M. Petzold, M.R. Phillips, D. Pope, C.A. Pope, J. Powles, M. Rao, H. Razavi, E.A. Rehfuess, J.T. Rehm, B. Ritz, F.P. Rivara, T. Roberts, C. Robinson, J.A. Rodriguez-Portales, I. Romieu, R. Room, L.C. Rosenfeld, A. Roy, L. Rushton, J.A. Salomon, U. Sampson, L. Sanchez-Riera, E. Sanman, A. Sapkota, S. Seedat, P. Shi, K. Shield, R. Shivakoti, G.M. Singh, D.A. Sleet, E. Smith, K. R. Smith, N.J.C. Stapelberg, K. Steenland, H. Stöckl, L.J. Stovner, K. Straif, L. Straney, G.D. Thurston, J.H. Tran, R. Van Dingenen, A. Van Donkelaar, J. L. Veerman, L. Vijayakumar, R. Weintraub, M.M. Weissman, R.A. White, H. Whiteford, S.T. Wiersma, J.D. Wilkinson, H.C. Williams, W. Williams, N. Wilson, A.D. Woolf, P. Yip, J.M. Zielinski, A.D. Lopez, C.J.L. Murray, M. Ezzati, A comparative risk assessment of burden of disease and injury attributable to 67 risk factors and risk factor clusters in 21 regions, 1990–2010: a systematic analysis for the Global Burden of Disease Study 2010, Lancet (2012), https://doi.org/10.1016/S0140-6736(12)61766-8.

[24] P.K. Lim, S.C. Ng, W.A. Jassim, S.J. Redmond, M. Zilany, A. Avolio, E. Lim, M. P. Tan, N.H. Lovell, Improved measurement of blood pressure by extraction of characteristic features from the cuff oscillometric waveform, Sensors (Switzerland) (2015), https://doi.org/10.3390/s150614142.

[25] S.H. Nam, P.J. Jeon, S.W. Min, Y.T. Lee, E.Y. Park, S. Im, Highly sensitive non-classical strain gauge using organic heptazole thin-film transistor circuit on a flexible substrate, Adv. Funct. Mater. 24 (2014) 4413–4419, https://doi.org/10.1002/adfm.201400139.

[26] M.L. Hammock, A. Chortos, B.C.K. Tee, J.B.H. Tok, Z. Bao, 25th anniversary article: the evolution of electronic skin (E-skin): a brief history, design considerations, and recent progress, Adv. Mater. 25 (2013) 5997–6038, https://doi.org/10.1002/adma.201302240.

[27] Y. Hu, C. Xu, Y. Zhang, L. Lin, R.L. Snyder, Z.L. Wang, A nanogenerator for energy harvesting from a rotating tire and its application as a self-powered pressure/speed sensor, Adv. Mater. 23 (2011) 4068–4071, https://doi.org/10.1002/adma.201102067.

[28] Q. Liu, J. Chen, Y. Li, G. Shi, High-performance strain sensors with fish-scale-like graphene-sensing layers for full-range detection of human motions, ACS Nano 10 (2016) 7901–7906, https://doi.org/10.1021/acsnano.6b03813.

[29] A.T. Sepúlveda, R. Guzman de Villoria, J.C. Viana, A.J. Pontes, B.L. Wardle, L. A. Rocha, Full elastic constitutive relation of non-isotropic aligned-CNT/PDMS flexible nanocomposites, Nanoscale. 5 (2013) 4847, https://doi.org/10.1039/c3nr00753g.

[30] D.J. Lipomi, M. Vosgueritchian, B.C.K. Tee, S.L. Hellstrom, J.A. Lee, C.H. Fox, Z. Bao, Skin-like pressure and strain sensors based on transparent elastic films of carbon nanotubes, Nat. Nanotechnol. 6 (2011) 788–792, https://doi.org/10.1038/nnano.2011.184.

[31] L. Wang, W. Dou, J. Chen, K. Lu, F. Zhang, M. Abdulaziz, W. Su, A. Li, C. Xu, Y. Sun, A CNT-PDMS wearable device for simultaneous measurement of wrist pulse pressure and cardiac electrical activity, Mater. Sci. Eng. C 117 (2020) 111345, https://doi.org/10.1016/j.msec.2020.111345.

[32] J. Bae, Y. Hwang, S. Park, J.-H. Ha, H. Kim, A. Jang, J. An, C.-S. Lee, S.-H. Park, Study on the sensing signal profiles for determination of process window of flexible sensors based on surface treated PDMS/CNT composite patches, Polymers (Basel) 10 (2018) 951, https://doi.org/10.3390/polym10090951.

[33] A.S. Zuruzi, T.M. Haffiz, D. Affidah, A. Amirul, A. Norfatriah, M.H. Nurmawati, Towards wearable pressure sensors using multiwall carbon nanotube/polydimethylsiloxane nanocomposite foams, Mater. Des. 132 (2017) 449–458, https://doi.org/10.1016/j.matdes.2017.06.059.

[34] X. Shuai, P. Zhu, W. Zeng, Y. Hu, X. Liang, Y. Zhang, R. Sun, C. Wong, Highly sensitive flexible pressure sensor based on silver nanowires-embedded polydimethylsiloxane electrode with microarray structure, ACS Appl. Mater. Interfaces 9 (2017) 26314–26324, https://doi.org/10.1021/acsami.7b05753.

[35] B. You, C.J. Han, Y. Kim, B.-K. Ju, J.-W. Kim, A wearable piezocapacitive pressure sensor with a single layer of silver nanowire-based elastomeric composite electrodes, J. Mater. Chem. A 4 (2016) 10435–10443, https://doi.org/10.1039/C6TA02449A.

[36] S. Baek, H. Jang, S.Y. Kim, H. Jeong, S. Han, Y. Jang, D.H. Kim, H.S. Lee, Flexible piezocapacitive sensors based on wrinkled microstructures: toward low-cost fabrication of pressure sensors over large areas, RSC Adv. 7 (2017) 39420–39426, https://doi.org/10.1039/C7RA06997A.

[37] Y. Joo, J. Byun, N. Seong, J. Ha, H. Kim, S. Kim, T. Kim, H. Im, D. Kim, Y. Hong, Silver nanowire-embedded PDMS with a multiscale structure for a highly sensitive and robust flexible pressure sensor, Nanoscale. 7 (2015) 6208–6215, https://doi.org/10.1039/C5NR00313J.

[38] C. Dagdeviren, Y. Su, P. Joe, R. Yona, Y. Liu, Y.-S. Kim, Y. Huang, A.R. Damadoran, J. Xia, L.W. Martin, Y. Huang, J.A. Rogers, Conformable amplified lead zirconate titanate sensors with enhanced piezoelectric response for cutaneous pressure monitoring, Nat. Commun. 5 (2014) 4496, https://doi.org/10.1038/ncomms5496.

[39] J. Chun, K.Y. Lee, C.-Y. Kang, M.W. Kim, S.-W. Kim, J.M. Baik, Embossed hollow hemisphere-based piezoelectric nanogenerator and highly responsive pressure

sensor, Adv. Funct. Mater. 24 (2014) 2038–2043, https://doi.org/10.1002/adfm.201302962.
[40] C. Pan, L. Dong, G. Zhu, S. Niu, R. Yu, Q. Yang, Y. Liu, Z.L. Wang, High-resolution electroluminescent imaging of pressure distribution using a piezoelectric nanowire LED array, Nat. Photonics 7 (2013) 752–758, https://doi.org/10.1038/nphoton.2013.191.
[41] L. Persano, C. Dagdeviren, Y. Su, Y. Zhang, S. Girardo, D. Pisignano, Y. Huang, J. A. Rogers, High performance piezoelectric devices based on aligned arrays of nanofibers of poly(vinylidenefluoride-co-trifluoroethylene), Nat. Commun. 4 (2013) 1633, https://doi.org/10.1038/ncomms2639.
[42] W. Choi, J. Lee, Y. Kyoung Yoo, S. Kang, J. Kim, J. Hoon Lee, Enhanced sensitivity of piezoelectric pressure sensor with microstructured polydimethylsiloxane layer, Appl. Phys. Lett. 104 (2014) 123701, https://doi.org/10.1063/1.4869816.
[43] M. Akiyama, Y. Morofuji, T. Kamohara, K. Nishikubo, M. Tsubai, O. Fukuda, N. Ueno, Flexible piezoelectric pressure sensors using oriented aluminum nitride thin films prepared on polyethylene terephthalate films, J. Appl. Phys. 100 (2006) 114318, https://doi.org/10.1063/1.2401312.
[44] C.-T. Lee, Y.-S. Chiu, Piezoelectric ZnO-nanorod-structured pressure sensors using GaN-based field-effect-transistor, Appl. Phys. Lett. 106 (2015), 073502, https://doi.org/10.1063/1.4910879.
[45] J.-H. Lee, H.-J. Yoon, T.Y. Kim, M.K. Gupta, J.H. Lee, W. Seung, H. Ryu, S.-W. Kim, Micropatterned P(VDF-TrFE) film-based piezoelectric nanogenerators for highly sensitive self-powered pressure sensors, Adv. Funct. Mater. 25 (2015) 3203–3209, https://doi.org/10.1002/adfm.201500856.
[46] C.-L. Choong, M.-B. Shim, B.-S. Lee, S. Jeon, D.-S. Ko, T.-H. Kang, J. Bae, S.H. Lee, K.-E. Byun, J. Im, Y.J. Jeong, C.E. Park, J.-J. Park, U.-I. Chung, Highly stretchable resistive pressure sensors using a conductive elastomeric composite on a micropyramid array, Adv. Mater. 26 (2014) 3451–3458, https://doi.org/10.1002/adma.201305182.
[47] H.K. Lee, J. Chung, S. Il Chang, E. Yoon, Real-time measurement of the three-axis contact force distribution using a flexible capacitive polymer tactile sensor, J. Micromech. Microeng. 21 (2011) 35010–35019, https://doi.org/10.1088/0960-1317/21/3/035010.
[48] B.-Y. Lee, J. Kim, H. Kim, C. Kim, S.-D. Lee, Low-cost flexible pressure sensor based on dielectric elastomer film with micro-pores, Sensors Actuators A Phys. 240 (2016) 103–109, https://doi.org/10.1016/j.sna.2016.01.037.
[49] A. Bijender, Kumar, one-rupee ultrasensitive wearable flexible low-pressure sensor, ACS Omega. 5 (2020) 16944–16950, https://doi.org/10.1021/acsomega.0c02278.
[50] D. Zhu, S. Handschuh-Wang, X. Zhou, Recent progress in fabrication and application of polydimethylsiloxane sponges, J. Mater. Chem. A 5 (2017) 16467–16497, https://doi.org/10.1039/c7ta04577h.
[51] S. Kumar, S. Bijender, A. Yadav, Kumar, flexible microhyperboloids facets giant sensitive ultra-low pressure sensor, Sensors Actuators A Phys. 328 (2021) 112767, https://doi.org/10.1016/j.sna.2021.112767.
[52] M. Forouzanfar, H.R. Dajani, V.Z. Groza, M. Bolic, S. Rajan, I. Batkin, Oscillometric blood pressure estimation: past, present, and future, IEEE Rev. Biomed. Eng. 8 (2015) 44–63, https://doi.org/10.1109/RBME.2015.2434215.
[53] W. Van Moer, L. Lauwers, D. Schoors, K. Barbè, Linearizing oscillometric blood-pressure measurements: (non)sense? IEEE Trans. Instrum. Meas. 60 (2011) 1267–1275, https://doi.org/10.1109/TIM.2010.2090703.
[54] Y. Jang, J. Jo, K. Woo, S.H. Lee, S. Kwon, H. Kim, H.S. Lee, Fabrication of highly sensitive piezocapacitive pressure sensors using a simple and inexpensive home milk frother, Phys. Rev. Appl (2019), https://doi.org/10.1103/PhysRevApplied.11.014037.